IEEE Access
Multidisciplinary ⋮ Rapid Review ⋮ Open Access Journal

Received 7 December 2022, accepted 13 February 2023, date of publication 6 March 2023, date of current version 24 April 2023.

Digital Object Identifier 10.1109/ACCESS.2023.3253542

APPLIED RESEARCH

Circularly Polarized Cross-Dipole Antenna for UHF RFID Readers Applicated in the Warehouse Environment

FULIN XUE[1], YIMING ZHANG[2], JUNLONG LI[3], AND HUI LIU[4], (Member, IEEE)

[1]Quectel Wireless Solutions Company Ltd., Foshan 528200, China
[2]Center for Optical and Electromagnetic Research, National Engineering Research Center for Optical Instruments, Zhejiang University, Hangzhou 310058, China
[3]Department of Oceanography, Shanwei Institute of Technology, Shanwei 516600, China
[4]School of Electronic and Information, Guangdong Polytechnic Normal University, Guangzhou 510665, China

Corresponding author: Hui Liu (liuhui@gpnu.edu.cn)

This work was supported in part by the Science and Technology Development Plans in Key Areas of Guangzhou 2022 Major Research Project under Grant 202206070001, and in part by the Talent Project of Guangdong Polytechnic Normal University under Grant 2021SDKYA055.

ABSTRACT In this paper, we proposed a broadband circularly polarized antenna with wide beamwidth. The main structure of the proposed antenna is a combined cross-polarized dipole antenna, four metal arms, a single coaxial cable and two feed structures with 90° phase delay. In order to attain a wide beamwidth antenna performance that can be used in a warehouse environment, we innovatively bent the metal arms and added a metal plane at a specific location to gain maximum beamwidth and the highest achievable gain. Especially, the application of metal bending arms not only reduce the space size of antenna, but also possess good axial ratio characteristic. The measurement illustrates that the antenna prototype achieves $S_{11} < -10$ dB impedance bandwidth (IBW) of 40% (820 - 1230 MHz), a 3-dB axial ratio bandwidth (ARBW) of 7.3% (895 - 970 MHz), and a maximum half-power beamwidth (HPBW) of 104° (@915 MHz). In addition, the good radiation characteristics of a gain of 6.33 dBic and an average radiation efficiency of 76.3% were measured in the operating bandwidth, which makes the proposed antenna a good candidate for the hasty logistics radio frequency identification (RFID) system.

INDEX TERMS Wide beamwidth, circular polarization (CP), single feed, cross-polarized dipole, folded metal arms, RFID.

I. INTRODUCTION

Circular polarized antenna is a popular area of research, due to its good ability to mitigate polarization mismatch and reduce multipath effect. CP antennas are widely used in RFID system, wireless local area network, satellite communication and GPS positioning and other areas [1], [2], [3]. To meet the application requirements in different scenarios, researchers are devoted to improve the performance of circularly polarized antennas like the axial ratio bandwidth and the lobe width, etc. by various technical solutions. The techniques, including using a slotting the radiation patch [1], a sequentially fed stacked CP patch [4], the quadrature feed networks [5], Wilkinson power splitter [6], [7] and balun bandpass filter [2], have been reported. However, these methods also bring some drawbacks, such as narrow bandwidth, narrow ARBW or HPBW, high cost, low utilization rate of plates, large loss, and so on. For the RFID system worked in the storage environment, more features, especially the performance between the tag and reader antennas, need to be concerned. Therefore, the common approach is setting up more than one reader with CP antennas to achieve a large range of reading and overcome the difficulty of large quantities of goods for effective management and statistics. Obviously, it is a challenge to design a circularly polarized antenna that can satisfy the requirements of wide beamwidth, high performance and low cost.

The associate editor coordinating the review of this manuscript and approving it for publication was Hussein Attia.

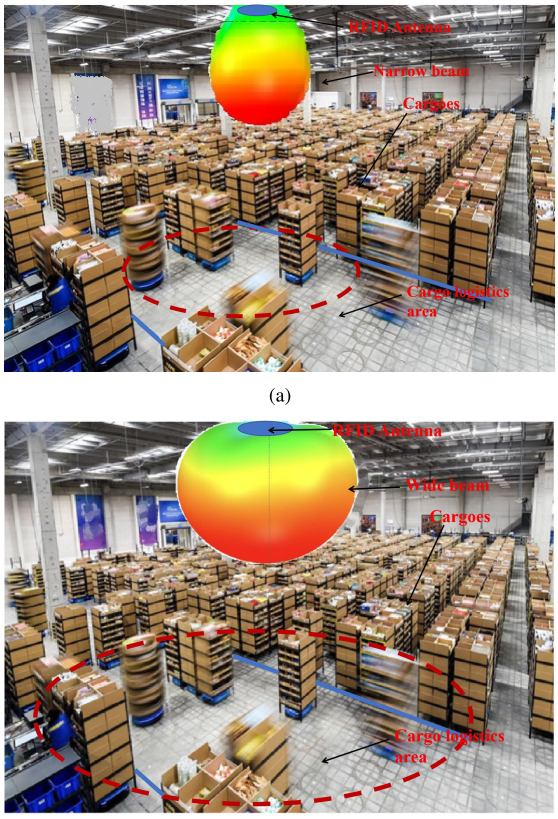

FIGURE 1. Warehouse environment diagram [8]. (a) The narrow beam antenna coverage scenario. (b) The wide beam antenna coverage scenario.

As shown in Fig. 1(a), it is evident that the narrow beamwidth antenna is difficult to cover all the cargoes in the logistics area, which will bring about narrow logistics channel, and slow logistics speed. Setting multiple antennas is a typical solution to be used to solve this problem, but this strategy will obviously increase the layout cost compared with use of wide beamwidth antenna in Fig. 1(b). Therefore, circularly polarized RFID reader antenna with wide beamwidth characteristic could be a better choice in the warehouse logistics environment. For the CP antennas, previous studies have found that, some CP radiation characteristics can be generated by the combination of two dipoles and a vacant quarter double-printed ring [3], [9], [10], [11]. In particular, the antenna in [3] applies an inverted L-shaped parasitic element with four sequential rotation angles to excite two additional CP modes. The IBW generated by the antenna is 91.4% (1.2 - 3.22 GHz), and the 3-dB ARBW is 74.1% (1.37 - 2.95 GHz). The Handheld Reader antenna [9] consists of two pairs of cross-dipoles fed by concentric ring-delay lines, achieves 3-dB ARBW of 882 - 936 MHz and 2.35 - 2.58 GHz. The dimension of the ground plane in [12] was reduced by adding a vertical ring at edge of the circular ground plane, The gain of the CP antenna is 8.7 dBic, and the HPBW < 65° at 880 MHz. In [13], the reported antenna is excited with a capacitively loaded (square ring slot) technique to cover the UHF RFID band, the IBW of 12.68% (852.40 - 967.80 MHz), and the HPBW of 86.20° at 910 MHz.

Under the condition of ensuring the performance of the polarization of the reader antenna in the RFID system, the radiation pattern and its dimension are both very concerned. In references [2], [11], [14], [15], the reflectors or reflection cavities were employed to improve the gain and the beamwidth for these antennas. But these assemblies also directly lead to the increase of the overall size of the reader antennas, which are $1.03\lambda_0 \times 1.03\lambda_0 \times 0.27\lambda_0$ (at 2.8 GHz), $1.01\ \lambda_0 \times 1.01\lambda_0 \times 0.29\lambda_0$ (at 2.17 GHz), $1.32\ \lambda_0 \times 1.32\lambda_0 \times 0.65\lambda_0$ (@2.49 GHz), $1.03\ \lambda_0 \times 1.03\lambda_0 \times 0.26\lambda_0$ (@2.57 GHz), respectively. Where λ_0 is the wavelength at the center frequency of the operating band. For this reason, planarized artificial magnetic conductor (AMC) has been invented to improve the performance of radiation pattern and maintain a relative compact size. In [16], the peak gain of the antenna increases from -1.31 dBic (without AMC) to 4.6 dBic (with AMC) at 900 MHz, but the IBW is 850 - 950 MHz, and the 3-dB ARBW is 2.2% (890 - 910 MHz). However, AMC is traditionally not an attractive option due to its relative narrow operating bandwidth and requiring a separate design process.

This paper presents a circularly polarized wideband antenna with a wide-beamwidth directional radiation, which has the advantages of small size, low cost, simple assembly and easy fabrication. In the warehouse environment, wide beamwidth CP antenna can cover a wider range of cargoes and reduce the number of reader Settings. In the design process, by bending the metal arms, the effective coverage area of the antenna can be increased appropriately and the upper part size of proposed antenna can also be reduced. Furthermore, a simple reflective surface manufactured by metal plate is strategically placed under the radiator to further widen the beamwidth and obtain the optimal gain. Simulation and experimental results demonstrate that the proposed method has the advantages of wide beamwidth, stable gain, better impedance and ARBW, which can be practically used in CP RFID reader for warehouse environment.

II. ANTENNA DESIGN AND ANALYSIS

A. ANTENNA CONFIGURATION

In Fig. 2, the top view and side view of the optimized antenna are shown comprehensively. The geometry of the proposed antennaconsists of cross-dipole antenna, a metal plate reflector, a coaxial line and some structural parts (plastic rivets and carriages, see Fig. 2(a)). The feed plate's substrate is FR-4 (dielectric constant $\varepsilon_r = 4.3$, loss tangent $\tan\sigma = 0.02$, thickness $H_2 = 0.762$ mm). The main radiator of the proposed antenna is composed of four metal arms, which construct a group of cross-dipole antennas, and the metal arms are both bending to optimize the top space as well as the radiation pattern of the antenna. Subsequently, in order to generate a better circularly polarized characteristic, the vacant-quarter ring microstrip line (Fig. 2(b)) is placed in the center of the top side of the substrate, which is connected

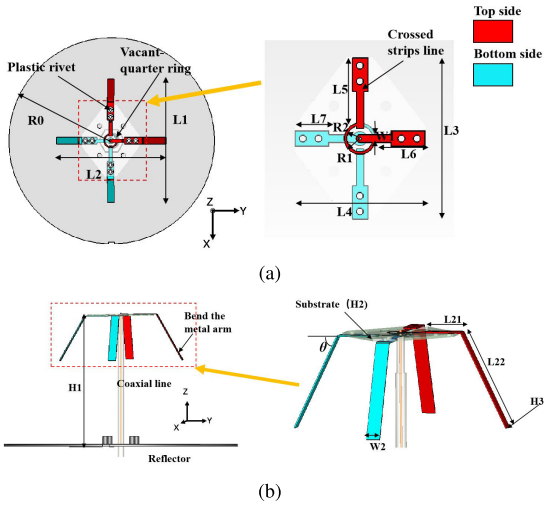

FIGURE 2. Geometry of the antenna. (a) Top view of the antenna. (b) Side view of the antenna.

TABLE 1. Geometric parameters of the designed antenna.

Parameter	Value	Parameter	Value
R_0	90 mm	L_7	13 mm
R_1	6 mm	L_{21}	16.4 mm
R_2	5 mm	L_{22}	39.5 mm
L_1	108 mm	W_1	2.9 mm
L_2	96 mm	W_2	6 mm
L_3	62.5 mm	H_1	100 mm
L_4	50.5 mm	H_2	0.762 mm
L_5	25.16 mm	H_3	0.5 mm
L_6	19.17 mm	θ	60°

to the metal arms through the strips line (see Fig. 2(a)), and generate a fixed phase difference between the metal are arm radiators. The feeding network (including the vacant-quarter ring and crossed strips line) is placed on the bottom side of the substrate in the same way to yield phase differences of 0°, 90°, 180°, 270° for the four metal arms, respectively. The final optimized structural parameters are shown in Table 1.

B. ANTENNA MECHANISM AND STRUCTURE EVOLUTION

The equivalent circuit model of the proposed antenna is shown in Fig. 3. In order to generate circularly polarized radiation, each vibration structure in the antenna must have equal power input and the phase difference between the input currents is 90°. Fig. 3(b) shows the impedance analysis of the dipole. It can be concluded that when $0 < L < 0.25\lambda_0$, the reactance part is less than zero, is capacitive, current phase advance. When $0.25\lambda_0 < L < 0.4\lambda_0$, the reactance part is greater than zero, presenting a perceptual, current phase lag. It is fed directly from the coaxial line, and adopts 1/4 phase shift structure to carry on the balance and unbalance feed conversion. Two groups of metal arms can be regarded as two admittances in parallel in the circuit model. In addition, because the two groups of metal arms are on the two planes, changing the length of one group arms is a high-speed and

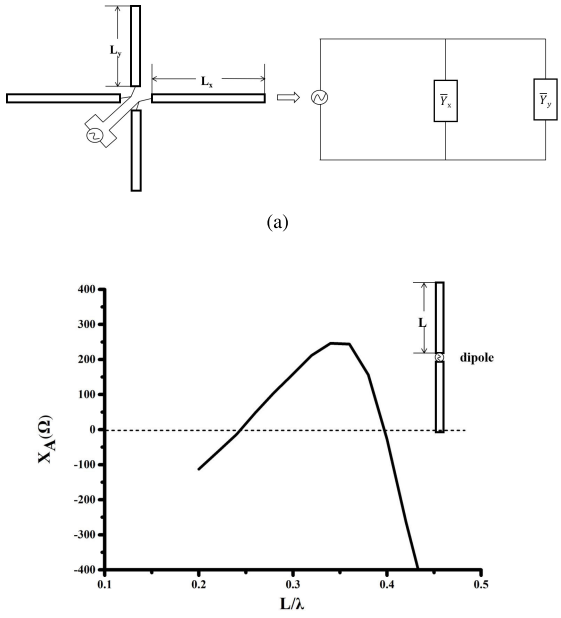

FIGURE 3. Equivalent circuit. (a) Equivalent circuit model for the proposed antenna. (b) Oscillator length and reactance curve.

effective tactic to obtain the optimal results of characteristics of circular polarization radiation in the far field.

Based on the proposed circuit theoretical model, we can vaguely preset two groups of metal arms with equal length, then the antenna model with circular polarization characteristic can be obtained rapidly through the optimization of commercial software CST. The antenna structure evolution is demonstrated in Fig. 4. First of all, we built the first prototype antenna Ant1: a group of cross-dipole antennas mounted on the PCB. In this step, the feeding network including the vacant-quarter ring microstrip lines and crossed strips line need to be designed first by using CST. Besides, a circular reflector metal plate with radius R_0 is set at H_1 below the radiator as the ground, the distance from the radiator to the metal plate reflector thus should be preliminarily determined at this step. Obviously, it's hard to optimize the dimension and radiation due to the fixed radiators of Ant1 (see Fig. 4(a)). According to Fig. 4, in order to explore the compact design, the metal arms were used to reduce the size of the PCB. Ant2 can obtain the same AR and S11 results as Ant1, but the size of the cell has been increased from 142 mm to 146 mm due to the reduction of the medium material (see Fig. 4(b)). The most important problem is that the circular polarization bandwidth is not working in the set frequency band (the IBW is 810-1180 MHz and the ARBW is 800-835 MHz), so the antenna does not have circular polarization characteristics.

The flexible metal arms provide possibility for further optimization. Subsequently, as shown in Fig. 4(c), the PCB feeding network is changed to unequal length ($L_3 \neq L_4$), so that the antenna is unequal width ($L_1 \neq L_2$). The adjacent arms of the long oscillator and the short oscillator are

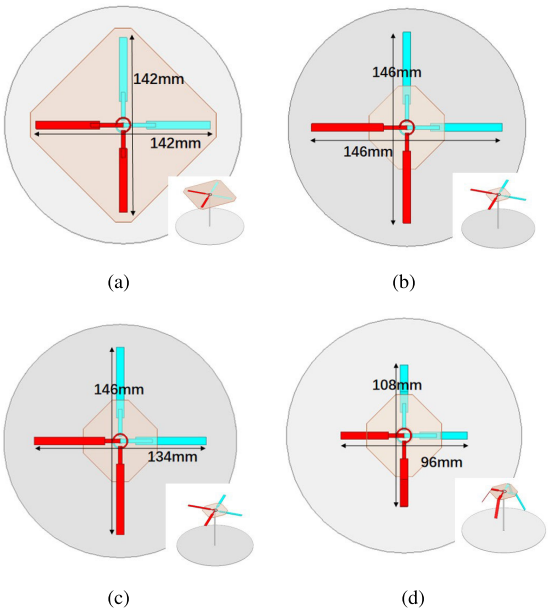

FIGURE 4. Four antenna structures in the design process. (a) Ant1: a group of cross-dipole antennas mounted on the PCB. (b) Ant2: Metal arms and PCB power splitter combined antenna. (c) Ant3: Combined antenna with flexible metal arms and PCB power splitter of unequal length. (d) Ant4: Integrated antenna with metal arms of bending and PCB power splitter of unequal width.

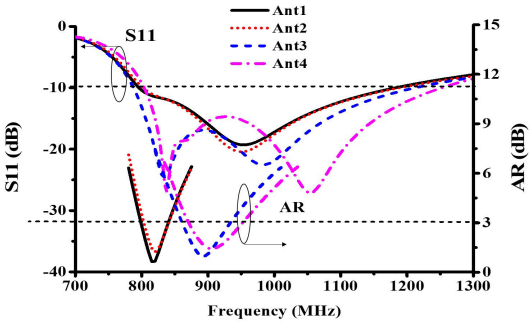

FIGURE 5. S_{11} and AR curves for different antennas.

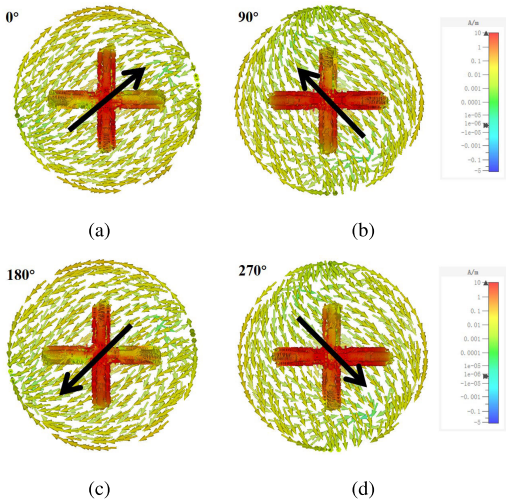

FIGURE 6. Simulated current distributions on the components of the optimized antenna at 0.915 GHz. (a) $\omega t = 0°$. (b) $\omega t = 90°$. (c) $\omega t = 180°$.(d) $\omega t = 270°$.

welded together, and the length of the oscillator is adjusted to obtain the phase difference, and the degenerate mode of aimed operating frequency band is generated to form circular polarization. The antenna thus excited another resonant point at 985 MHz, and the IBW was further expanded to 792-1213 MHz and the ARBW was corrected from 800-835MHz to 861-934 MHz.Therefore, the antenna has circular polarization characteristics in the RFID working band. However, These three structures have one problem in common: the overall volume of the antennas are too large to be applicated in the warehousing and logistics environment. Finally, in Fig. 4(d), we bent the four metal arms to save the volume of the top of the antenna to construct the Ant4, the optimized dimension is only 0.33 $\lambda_0 \times$ 0.29λ_0 at 915 MHz. Moreover, it should be noted that the bending angle of the metal arm θ is a key parameter for our antenna design, which can significantly impact the beam width and the IBW of the antenna. These contents will be discussed and analyzed in the next section. Also in Fig. 5, the optimal result of our design demonstrated that the IBW and the ARBW has been increased to 820 - 1230 MHz and 873-960 MHz, respectively, which completely covers the international common UHF RFID frequency band.

Fig. 6 presents the simulated current distribution on the bending metal arms. At 915 MHz, the vertical metal arms have the maximum current at $t = 0$T, while the horizontal arms display the maximum current at $t = $ T/4. At $t = $ T/2 and $t = 3$T/4, the direction of the current is opposite to that at $t = 0$T and $t = $ T/4 respectively (T denotes the period of oscillation at each frequency). When ωt is 0°, 90°, 180° and 270°, the synthetic current at 915 MHz frequency points to 45°, 135°, 225° and 315° directions, respectively. The resulting current vector sum flows in a counter clockwise direction. Consequently, the variation of surface current distribution with time mainly leads to right-handed circular polarization (RHCP) radiation in the Z > 0 half-space.

C. ANTENNA PARAMETER ANALYSIS

The IBWs and ARBWs of different lengths of metal bending arm (L_{22}) are pictured in Fig. 7. It's clear that a variation of length L_{22} will directly affect the operating band as the electrical length of the antenna change. The dimension parameters of the microstrip structures of the feed plate directly affect the impedance matching of the circular-polarized antenna, hence the parameters of vacant-quarter double-printed ring radius (R_1) and feed microstrip width (W_1) are exhibited in Fig. 8. It can be clearly seen that the change in R_1 is related to the impedance matching of the high frequency part. When R_1 gradually decreases, the impedance bandwidth for the high frequency part will be widened. In addition, the resonance of the proposed antenna becomes stronger when parameter W_1

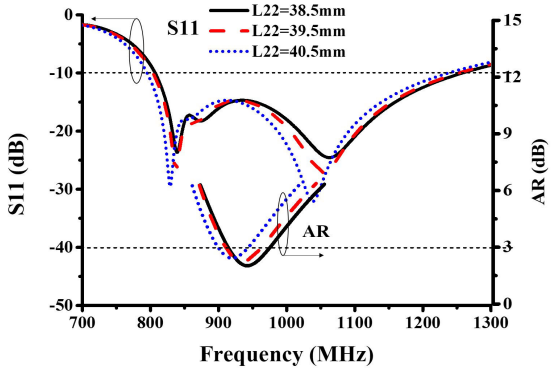

FIGURE 7. Simulated S_{11} and AR versus the frequency with different dimensions of L_{22}.

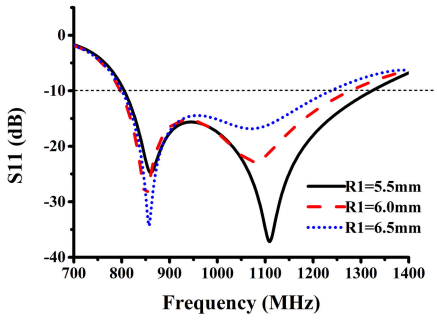

(a)

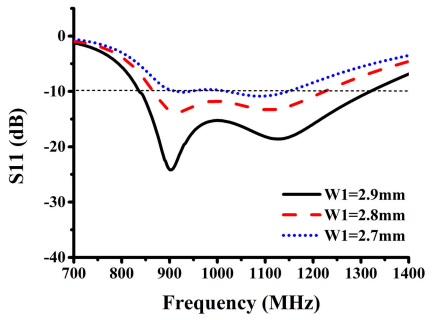

(b)

FIGURE 8. S_{11} of the proposed antenna with different parameters. (a) R_1. (b) W_1.

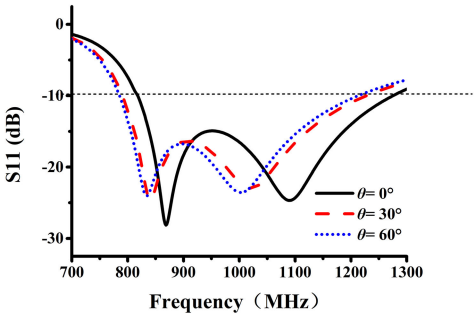

(a)

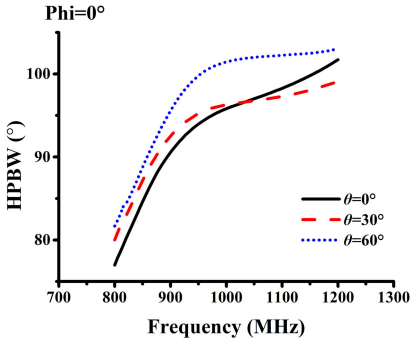

(b)

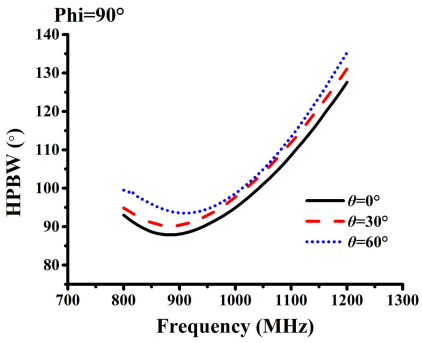

(c)

FIGURE 9. Simulated S_{11} and HPBW versus the frequency with different dimensions of θ. (a) S_{11}. (b) HPBW (Phi = 0°). (c) HPBW (Phi = 90°).

increasing from 2.7 mm to 2.9 mm, which is caused by the change of the impedance at the feeding position.

To describe the influence of different bending angles θ of the metal arm on IBW and HPBW, these simulation results corresponding to $\theta = 0°$, 30° and 60° are exhibited in Fig. 9(a) - (c). With the increase of bending Angle θ, the IBW changes from 785-1216 MHz to 820-1260 MHz. At the frequency point of 915 MHz, the HPBW is 91°(Phi = 0°) and 87°(Phi = 90°) when $\theta = 0°$. Obviously, the HPBW increases to 97°(Phi = 0°) and 96°(Phi = 90°) when $\theta = 60°$. In other frequency bands, the beamwidth of the wave has also increased significantly. Through these data analysis, the HPBW can be improved by above method. Then we investigated the optimal distance (H_1) between the radiators and reflector, as well as changing the size (R_0) of the reflector. it is found that with the change of radius R_0, the performance of IBW changes very little. However, as shown in Fig. 10, the best 3-dB ARBW can reach (897-960MHz) when $R_0 = 90$mm. In Fig. 11(a) - (d), it can be concluded that the IBW broadens slightly but the HPBW of the antenna is significantly widened as H_1 increasing from 90 mm to 110 mm. At the frequency point of 915 MHz, the HPBW increases from 93°(Phi = 0°), 88°(Phi = 90°) to 100°(Phi = 0°), 100°(Phi = 90°) (see Fig. 11(c)-(d)). Although the beamwidth is improved obviously, but the maximum gain is reduced from 6.5 dBic to 5.8 dBic in Fig. 11(b). It can be easily found that the higher the operating band, the bigger the difference of simulated results in the high frequency band.

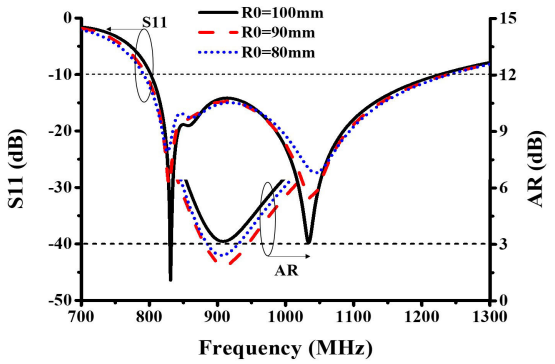

FIGURE 10. Simulated S_{11} and AR versus the frequency with different dimensions of R_0.

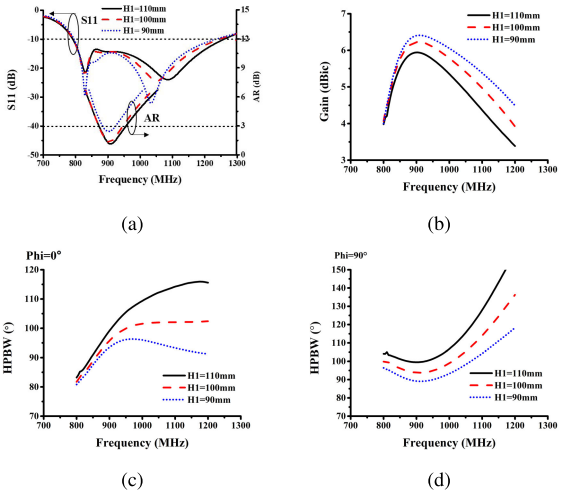

FIGURE 11. Simulated performance versus the frequency with different dimensions of H_1. (a)S_{11} and AR. (b) Gain. (c)HPBW (Phi = 0°). (d) HPBW (Phi = 90°).

Considering all aspects of performance, $H_1 = 100$mm was finally selected.

D. COMPARISON WITH PREVIOUS WORK

In order to explain the excellent performances of the proposed antenna, Table 2 explicates the contrast between the previous CP antennas and the antenna in this paper. It is obvious that a maximum HPBW achieved in our design, which reaches 104° at 915 MHz operating frequency point and significantly exceeds that of other reported literatures. Besides, the overall dimension and radiators (unit cell) size both have distinct advantage. Although our design has relatively low peak gain, which is caused by the smaller radiator and greater spatial energy distribution, it has been confirmed to operate effectively in our application environment. Moreover, the 3-dB axial ratio bandwidth of our design is not so prominent, but the impedance bandwidth is significantly greater than other reported circularly polarized antennas.

III. EXPERIMENTAL RESULTS AND DISCUSSIONS

Referring to Fig. 12(a) - (c), we fabricated and measured the CP cross-dipole antenna to verify the accuracy of the optimized design. As shown in Fig. 13, the measured results of S_{11} and AR are 40%(820 - 1230 MHz) and 7.3% (895 - 970 MHz) respectively, which are basically consistent with

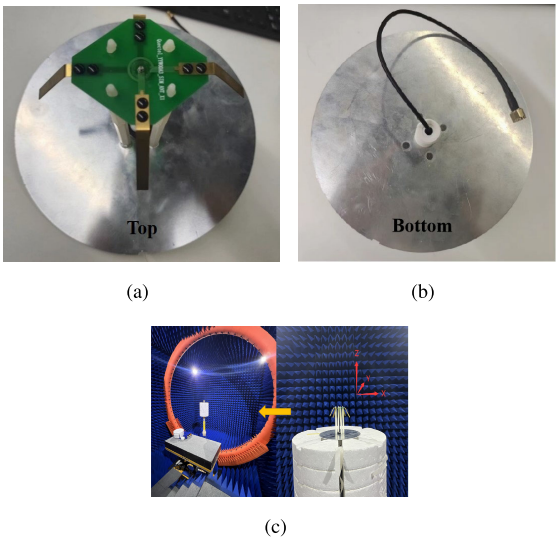

FIGURE 12. Photograph of the antenna prototype and test environment. (a) Top of the fabricated antenna. (b) Bottom of the fabricated antenna. (c) Measurement setup in an anechoic chamber.

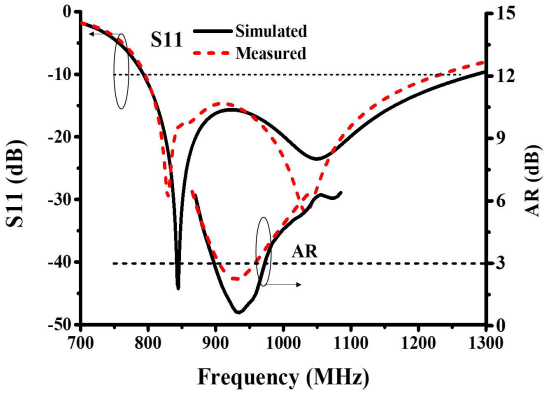

FIGURE 13. Simulated and measured S_{11} of the proposed antenna.

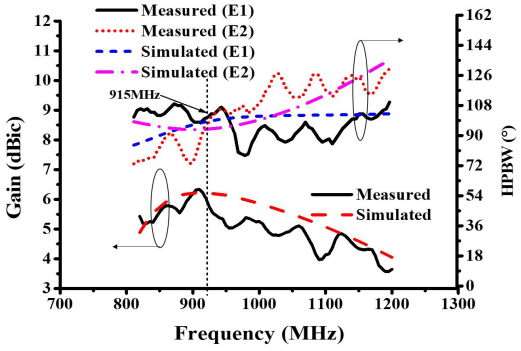

FIGURE 14. Simulated and measured of RHCP gains and HPBW versus the frequency.

TABLE 2. Comparison of the LWA proposed in this paper with previously published CP LWAs.

Reference	10dB IBW, %	3-dB ARBW, %	Size (λ_0^3)	Max Gain (dBic)	Unit cell Size (λ_0^2)	Max HPBW (915 MHz)
[12]	845 - 960 MHz, 12.8	840 - 965 MHz, 13.8	0.61 × 0.61 × 0.15	8.9	0.44 × 0.44	62°
[13]	852 - 968 MHz, 12.7	858 - 962 MHz, 11.4	0.46 × 0.46 × 0.13	6.2	0.44 × 0.44	86°
[20]	884 - 932 MHz, 5.3	890 - 934 MHz, 4.8	0.73 × 0.73 × 0.33	9.8	0.41 × 0.41	75°
[21]	833 - 960 MHz, 14.1	846 - 926MHz, 9.0	0.45 × 0.45 × 0.074	7.3	0.45 × 0.45	77°
Our work	820 - 1230MHz, 40	895 - 970MHz, 7.3	0.54 × 0.54 × 0.30	6.3	0.33 × 0.29	104°

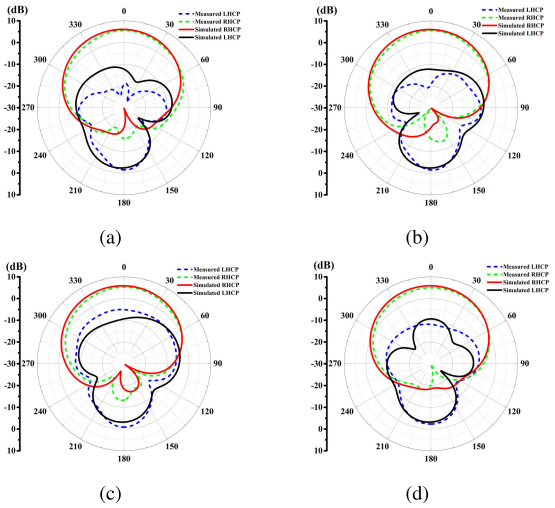

FIGURE 15. Simulated and measured normalized radiation patterns of the proposed CP dipole antenna at: (a) 900 MHz xz-plane. (b) 900 MHz yz-plane. (c) 960 MHz xz-plane. (d) 960 MHz yz-plane. (dotted lines are the measured results and solid lines are the simulated results).

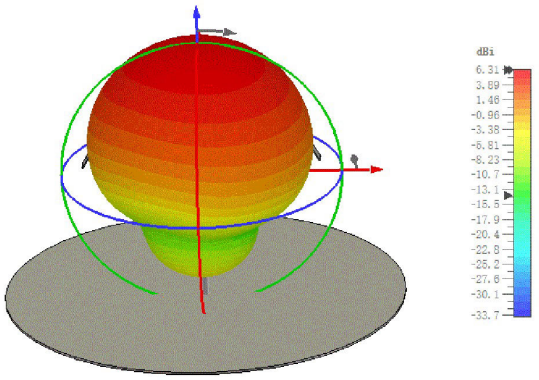

FIGURE 16. Simulated 3D radiation gain pattern.

the simulation results. It should be noted that although the measured data shown in Fig. 14 has fluctuations, which are mainly caused by fewer test frequency points and some errors in test and fabrication process. The overall trend demonstrates that the beamwidth of the proposed antenna is still characterized by a wide beamwidth. Some unavoidable errors in dielectric constant of the substrate, processing tolerance and measurement lead slight errors in the measurement results of the high-frequency part, but these unexcepted results are acceptable for our design. The measured gain and HPBW are 6.3 dBic (6.2 dBic in simulation) and 104° (100° in simulation) at 915 MHz, respectively. The measured efficiency is 76.3%. In addition, the simulated and measured directions at 900 MHz and 960 MHz are plotted in Fig. 15(a) - (d), the results exhibits that a stable radiation pattern can be obtained in the whole operating band. The simulation result also shows that the radiation field of the antenna is good in Fig. 16, and the radiation pattern of RHCP is consistent with the expectation.

IV. CONCLUSION

A wideband circularly polarized antenna with wide beamwidth radiation is presented. A vacant quarter double-printed ring and four bent metal arms are used to realize a CP radiation and wide beam. With four bended arms, the dimension of the antenna effectively reduced to yield a better HPBW without worsening the IBW as well as the circular polarization characteristic. Finally, a wider beamwidth and maximum gain can be achieved by optimizing the reflector. The verification prototype is fabricated and measured. The measurement results demonstrate that the IBW is 820 - 1230 MHz, the 3-dB ARBW is 895 - 970 MHz, and the maximum HPBW is 104° (@915 MHz) with a peak gain of 6.33 dBic. At the same time, the efficiency was 76.3%. With these attractive features, the antenna could be an ideal candidate for warehousing and logistics, as well as for other communication systems.

REFERENCES

[1] S. Wu, J. Yuan, J. Chen, and Y. Li, "Compact circularly polarized microstrip ring antenna using capacitive coupling structure for RFID readers," *IEEE Access*, vol. 8, pp. 32617–32623, 2020, doi: 10.1109/ACCESS.2020.2973719.

[2] C.-Q. Feng, F.-S. Zhang, and F.-K. Sun, "A broadband crossed dipole antenna with wide axial ratio beamwidth for satellite communications," *Prog. Electromagn. Res. Lett.*, vol. 77, pp. 59–64, 2018.

[3] L. Wang, W.-X. Fang, Y.-F. En, Y. Huang, W.-H. Shao, and B. Yao, "Wideband circularly polarized cross-dipole antenna with parasitic elements," *IEEE Access*, vol. 7, pp. 35097–35102, 2019, doi: 10.1109/ACCESS.2019.2904658.

[4] Z. N. Chen, X. Qing, and H. L. Chung, "A universal UHF RFID reader antenna," *IEEE Trans. Microw. Theory Techn.*, vol. 57, no. 5, pp. 1275–1282, May 2009, doi: 10.1109/TMTT.2009.2017290.

[5] L. Wen, S. Gao, Q. Luo, W. Hu, and B. Sanz-Izquierdo, "Design of a wideband dual-feed circularly polarized antenna for different axial ratio requirements," *IEEE Antennas Wireless Propag. Lett.*, vol. 20, no. 1, pp. 88–92, Jan. 2021, doi: 10.1109/LAWP.2020.3041362.
[6] D.-J. Wei, J. Li, J. Liu, G. Yang, and W. Zhang, "Dual-band substrate-integrated waveguide leaky-wave antenna with a simple feeding way," *IEEE Antennas Wireless Propag. Lett.*, vol. 18, no. 4, pp. 591–595, Apr. 2019.
[7] K. M. Mak and K. M. Luk, "A circularly polarized antenna with wide axial ratio beamwidth," *IEEE Trans. Antennas Propag.*, vol. 57, no. 10, pp. 3309–3312, Oct. 2009, doi: 10.1109/TAP.2009.2029370.
[8] [Online]. Available: https://www.rackwms.com/rack/335.html
[9] F.-P. Lai, J.-F. Yang, and Y.-S. Chen, "Compact dual-band circularly polarized antenna using double cross dipoles for RFID handheld readers," *IEEE Antennas Wireless Propag. Lett.*, vol. 19, no. 8, pp. 1429–1433, Aug. 2020, doi: 10.1109/LAWP.2020.3004881.
[10] X. Yang, J. Yuan, and G. Han, "Compact circularly polarized crossed dipole antenna with chip inductors and square rings loading for GPS applications," *Prog. Electromagn. Res. Lett.*, vol. 58, pp. 29–35, 2016, doi: 10.2528/PIERL15111909.
[11] Y. Li, Z. Zhao, J. Liu, and Y.-Z. Yin, "A cavity-backed wideband circularly polarized crossed bowtie dipole antenna with sequentially rotated parasitic elements," *Prog. Electromagn. Res. Lett.*, vol. 79, pp. 1–7, 2018, doi: 10.2528/PIERL18080802.
[12] H. F. Hammad, "High gain circularly polarized stacked circular patches loaded with a circular sector notches and vertical ground ring for UHF RFID universal reader," in *Proc. IEEE Int. Symp. Antennas Propag. USNC-URSI Radio Sci. Meeting*, Jul. 2019, pp. 1087–1088, doi: 10.1109/APUSNCURSINRSM.2019.8889005.
[13] K. Boonying and E. Nugoolcharoenlap, "Unidirectional circularly polarized elliptical flat antenna for UHF RFID reader," in *Proc. 21st Int. Symp. Wireless Pers. Multimedia Commun. (WPMC)*, Nov. 2018, pp. 31–34, doi: 10.1109/WPMC.2018.8713134.
[14] G. Liu, L. Xu, and Z.-S. Wu, "Miniaturized crossed-dipole circularly polarized fractal antenna," *Prog. Electromagn. Res. Lett.*, vol. 39, pp. 49–62, 2013, doi: 10.2528/PIERL13020507.
[15] S.-W. Qu, C. H. Chan, and Q. Xue, "Wideband and high-gain composite cavity-backed crossed triangular bowtie dipoles for circularly polarized radiation," *IEEE Trans. Antennas Propag.*, vol. 58, no. 10, pp. 3157–3164, Oct. 2010, doi: 10.1109/TAP.2010.2055792.
[16] C. Bajaj, D. K. Upadhyay, S. Kumar, and B. K. Kanaujia, "Circularly polarized cross-dipole antenna with a double layer AMC backing for UHF RFID readers," in *Proc. Int. Conf. Commun., Control Inf. Sci. (ICCISC)*, Vol. 1, Jun. 2021, pp. 1–4, doi: 10.1109/ICCISC52257.2021.9484947.
[17] Z. Wang, Y. Dong, and T. Itoh, "Metamaterial-based, miniaturised circularly polarised antennas for RFID application," *IET Microw., Antennas Propag.*, vol. 15, no. 6, pp. 547–559, May 2021, doi: 10.1049/mia2.12064.
[18] B.-S. Chen and C.-Y.-Y. Sim, "Broadband circularly polarized stacked patch antenna for universal UHF RFID applications," in *Proc. Int. Symp. Antennas Propag. Conf.*, Dec. 2014, pp. 99–100, doi: 10.1109/ISANP.2014.7026549.
[19] S. Konjunthes, S. Chalermwisutkul, P. Akkaraekthalin, and W. Thaiwirot, "Design and experiment of a wideband circularly polarized stacked patch antenna for universal UHF RFID readers," in *Proc. Res., Invention, Innov. Congr., Innov. Elect. Electron. (RIC)*, 2021, pp. 135–138, doi: 10.1109/RI2C51727.2021.9559830.
[20] Y. Pan and Y. Dong, "Circularly polarized stack Yagi RFID reader antenna," *IEEE Antennas Wireless Propag. Lett.*, vol. 19, no. 7, pp. 1053–1057, Jul. 2020, doi: 10.1109/LAWP.2020.2987936.
[21] J. Li, H. Liu, S. Zhang, M. Luo, Y. Zhang, and S. He, "A wideband single-fed, circularly-polarized patch antenna with enhanced axial ratio bandwidth for UHF RFID reader applications," *IEEE Access*, vol. 6, pp. 55883–55892, 2018, doi: 10.1109/ACCESS.2018.2872692.
[22] S. X. Ta, I. Park, and R. W. Ziolkowski, "Broadband electrically small circularly polarized directive antenna," *IEEE Access*, vol. 5, pp. 14657–14663, 2017, doi: 10.1109/ACCESS.2017.2730236.
[23] S. X. Ta, "Polarizations of crossed-dipole antenna loaded with different NFRP elements," *Prog. Electromagn. Res. M*, vol. 75, pp. 131–140, 2018, doi: 10.2528/PIERM18092301.

FULIN XUE was born in Xinzhou, China. He received the M.E. degree from the Centre for Optical and Electromagnetic Research, South China Academy of Advanced Optoelectronics, South China Normal University, Guangzhou, China, in 2019. From 2019 to 2021, he was a RF Engineer with CICT Mobile Communication Technology Company Ltd., Wuhan, China. Since 2021, he has been a RF Engineer with Quectel Wireless Solutions Company Ltd., Foshan, China. His current research interests include microwave components, RF circuits, antennas, and arrays.

YIMING ZHANG was born in Xianyang, China. He received the B.S. degree in electronic science and technology from the Shaanxi University of Science and Technology, Xi'an, China, in 2016, and the M.S. degree in electromagnetic field and microwave technology from the Centre for Optical and Electromagnetic Research, South China Academy of Advanced Optoelectronics, South China Normal University, Guangzhou, China, in 2021. He is currently pursuing the Ph.D. degree with the Centre for Optical and Electromagnetic Research, Zhejiang University, Hangzhou, China. From 2021 to 2022, he was a RF Engineer with Xiaomi Communications Company Ltd., Shenzhen, China. His current research interests include microwave components, RF circuits, antennas, and arrays.

JUNLONG LI was born in Guangdong, China, in 1992. He received the M.E. degree from the Centre for Optical and Electromagnetic Research, South China Academy of Advanced Optoelectronics, South China Normal University, Guangzhou, China, in 2019. From 2019 to 2020, he was a RF Engineer with Huawei Communications Company Ltd., Dongguan, China. In 2020, he joined the School of Oceanography, Shanwei Institute of Technology, as a Faculty Member. His research interests include antenna, RF circuits, and the Internet of Things technology.

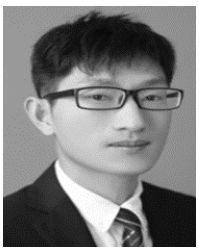

HUI LIU (Member, IEEE) was born in Zhumadian, China. He received the M.S. degree in electromagnetic field and microwave technology from South China Normal University, China, in 2013, and the Ph.D. degree in microelectronics and solid state electronics from the Centre for Optical and Electromagnetic Research, Academy of Advanced Optoelectronics, South China Normal University, in 2018. He was a Postdoctoral Researcher with the Center for Optical and Electromagnetic Research, Zhejiang University, from 2018 to 2020. In 2020, he joined the School of Electronic and Information, Guangdong Polytechnic Normal University, as a Faculty Member. His research interests include antenna, RF circuits, and microwave components.